



# Analysis of Ultra-Central Relativistic Heavy Ions Collisions Based on Energy Parameterization

Liner Santos<sup>1</sup>

Received: 5 September 2024 / Accepted: 12 September 2024 / Published online: 23 September 2024  
© The Author(s) under exclusive licence to Sociedade Brasileira de Física 2024

## Abstract

Hydrodynamic models of heavy-ion collisions have been very successful at describing experimental data. A peculiar exception is anisotropic flow in ultra-central collisions. No existing model for the initial stages of a heavy-ion collision, when used as initial conditions for hydrodynamics simulations, can provide a satisfactory description of flow in ultra-central collisions. It is therefore useful to understand what properties the initial stages must have in order to be compatible with experimental data. To this end, we parameterize the early-time energy density and its fluctuations via its 1-point and 2-point function and constrain them by using experimental data for  $v_{n2}$  in conjunction with hydrodynamic simulations. We find that it is possible to describe experimental data, but it requires larger fluctuations in regions of low density, as compared to existing Monte Carlo models. We comment on the implications of this finding, as well as the limitations of this initial analysis and how it can be improved in the future.

## 1 Introduction

In an ultra-relativistic heavy-ion collision, there is a large energy deposition, and we suppose that there is a “breakup” of the hadronic structure and the partons from participant nucleons are not confined anymore. That is, a phase transition<sup>1</sup> occurs to a system composed by free partons which behave as a strongly coupled fluid. This phase is called *Quark-Gluon Plasma - QGP*.

Due to the short duration of this phase, it is not possible to directly observe this phase of matter, and so conclusions are formulated about its behavior from the final characteristics, such as the multiplicity of charged hadrons and their azimuthal distribution, through the analysis of harmonic flows coefficients  $v_n$ . The latter can be related with the anisotropy of initial conditions, represented by *eccentricities*  $\epsilon_n$ . We will show throughout the text that  $\epsilon_2$  has geometric and fluctuation contributions, while  $\epsilon_3$  have nuclei fluctuations contributions only. Thus, we can think, for instance,

that  $v_3 < v_2$  and this result is true for most cases, as we can see in [1], for instance.

However, in ultra-central events, i.e., events within centrality bins, we observe results as  $v_3 \simeq v_2$  and no model could describe these results until now, as we can see in Fig. 1, from Luzum et al. [13]. Gianinni et al. [8] and Kuroki et al. [11] also discuss the emergence of this issue and show that no attempt can solve it until now. The fact that we have a triangular flow bigger than elliptic flow makes us think about the influence of the fluctuations and how it should be a model so that it generates the initial conditions which harmonic flows agree with experimental data. Thus, the present work aims to study if it is possible to describe the initial conditions in order that calculated harmonic flows be as close as possible to experimental data from ATLAS [1] at the LHC. For this purpose, we put constraints on the  $n$ -point functions that describe fluctuations of the initial energy density, according to Grönqvist et al. [9], in order to have a relationship between the fluctuations and the correlations and the initial conditions.

Besides, in this work, it is assumed that viscosities do not change along the system temperature. This is a naive approach but can serve as a starting point for studying these cases.

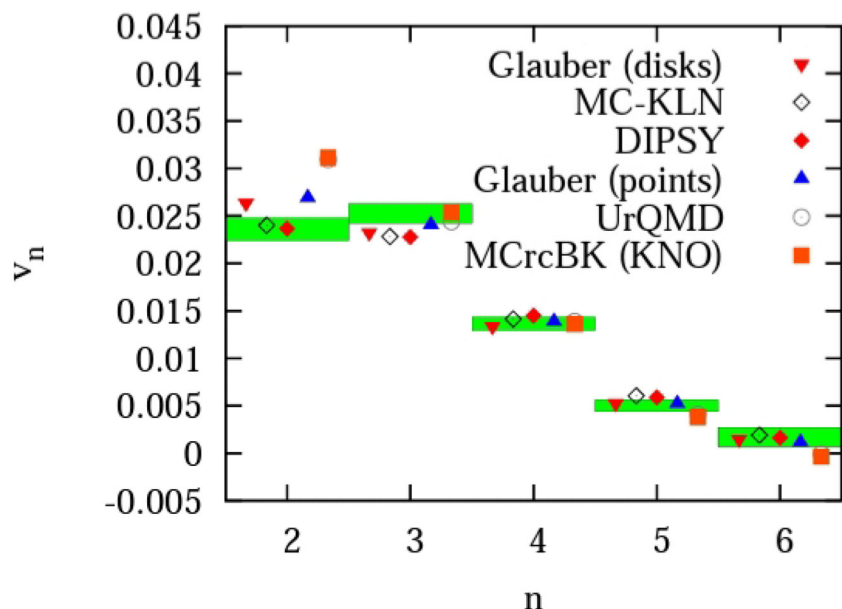
The fluctuations in the early-time density of the system are naturally characterized by its  $N$ -point correlation functions, as we can see in Grönqvist et al. [9]. In this work, we try to

<sup>1</sup> Calculus on lattice QCD shows a crossover, i.e., a smooth transition from hadron gas to QCD matter when baryon density is very low.

✉ Liner Santos  
linersantos@usp.br

<sup>1</sup> Instituto de Física, Universidade de São Paulo, R. do Matão 1371, 05508-090 São Paulo, SP, Brazil

**Fig. 1** Experimental values (green bars) of the ATLAS collaboration with centrality class 0 – 1% and the values obtained by several models proposed for  $v_n$ . Image from [13]



answer whether it is possible to describe the observables in this centrality regime, using the approach mentioned above.

To do this, we make use of the known relationships between final measured flow  $v_n$  and the initial spatial anisotropy  $\varepsilon_n$ , combined with relations between the latter and the  $N$ -point functions of the initial density of the system. By comparing to measured  $v_n\{2\}$  data in centralities of 0 – 1% or less, we thus constrain these fluctuations.

In Sec. 2, we review the formalism and the approximations employed in this work. In Sec. 3, we compute the required hydrodynamic response coefficients  $K_n \equiv v_n\{2\}/\varepsilon_n\{2\}$  over a wide range in parameter space. Finally, in Sec. 4, we make a comparison between measured data and parameterized fluctuations and determine the necessary values of fluctuation parameters.

## 2 N-point Function Formalism

The final momentum anisotropy of particles, as quantified in flow harmonics  $v_n$ , can be simply related to the spatial anisotropy of the system. A systematic expansion can be constructed from cumulants of the initial energy density in a given event, with lowest order terms representing the large scale structure, to which corrections that can be added as higher-order cumulants and higher powers of anisotropic cumulants. For central collision in particular, the lowest-order, linear relations form a good approximation [6]:

$$v_n \simeq K_n \varepsilon_n \quad (1)$$

$$\varepsilon_n = -\frac{\int d^2x \rho(\vec{x}) r^n e^{in\phi}}{\int d^2x \rho(\vec{x}) r^n} \quad (2)$$

Here,  $\varepsilon_n$  represents all the relevant properties of the initial state for describing harmonic  $n$  (and which fluctuates from event to event). The response coefficients  $K_n$ , on the other hand, contain all information about the medium that is created and the subsequent evolution of the system. It is constant within a centrality bin. Event-averaged observables from the final state (such as 2-particle cumulants  $v_n\{2\}$ ) can therefore be simply related to the initial state:

$$v_n\{2\} \equiv \sqrt{\langle |v_n|^2 \rangle} \quad (3)$$

$$\varepsilon_n\{2\} \equiv \sqrt{\langle |\varepsilon_n|^2 \rangle} \quad (4)$$

$$\implies v_n\{2\} \simeq K_n \varepsilon_n\{2\} \quad (5)$$

In Refs. [2, 9], the authors derived analytic expressions for RMS eccentricity  $\varepsilon_n\{2\}$ , which we make use of in this work. To summarize, we write the local energy density in the transverse plane in a single event as an average value plus a fluctuation:

$$\rho(\vec{x}) = \langle \rho(\vec{x}) \rangle + \delta\rho(\vec{x}) \quad (6)$$

Two important approximations are used to guide the derivation. First, we assume that the transverse distance over which fluctuations are correlated is much smaller than the overall transverse size of the system. In that case, we can ignore these correlations and approximate the system as delta-correlated, with local fluctuations. That is, the connected  $N$ -point correlators of the density  $\rho$  can be written as

$$\langle \rho(\vec{x}) \rangle = \kappa_1(\vec{x}) \quad (7)$$

$$\langle \delta\rho(\vec{x}_1) \delta\rho(\vec{x}_2) \rangle = \kappa_2(\vec{x}) \delta(\vec{x}_2 - \vec{x}_1) \quad (8)$$

$$\langle \delta\rho(\vec{x}_1)\delta\rho(\vec{x}_2)\delta\rho(\vec{x}_3) \rangle = \kappa_3(\vec{x})\delta(\vec{x}_2 - \vec{x}_1)\delta(\vec{x}_3 - \vec{x}_1) \quad (9)$$

:

and the useful information about fluctuations is contained in the functions  $\kappa_n$ , which describe the local fluctuations in the density of energy that is deposited near mid-rapidity in a particular centrality class. Our goal is to characterize what properties these functions must have in order to describe measured data in ultra-central collisions.

To obtain analytic expressions for RMS eccentricities, a series expansion is constructed in powers of the fluctuation  $\delta\rho$ . That is, an approximation of small fluctuations is made. To leading order in fluctuations, only the 1-point and 2-point functions contribute:

$$\varepsilon_n\{2\} = \sqrt{\frac{\int d^2x r_\perp^{2n} \kappa_2(\vec{x})}{(\int d^2x r_\perp^n \kappa_1(\vec{x}))^2}}, \quad (10)$$

while higher-order fluctuations  $\kappa_n$  appear at higher order in the power-series expansion. Here,  $r_\perp = \sqrt{x^2 + y^2}$  is the transverse radial coordinate.

To summarize, by making the approximation of small, local fluctuations, we can obtain an analytic expression of RMS eccentricities in terms of the local mean and variance of initial density fluctuations. In the following, we will be particularly interested in characterizing the fluctuations  $\kappa_2$  via a parameterization and comparison to experimental data.

### 3 Computing the Hydrodynamic Response

#### 3.1 The CGC Model

According to Lappi [12], this model can also be used to determine initial conditions and is mathematically similar to Glauber's optical model, according to which nucleons move independently of each other and in path linear tubes (called *flow tubes*). The term optical comes in the sense of saying what each nucleon "see" through the flux tube. The essential difference between CGC and Glauber is that the former refers to multiple events, while the Glauber model focuses on the results of a collision event. Furthermore, as mentioned previously, the CGC model proposes a description for the nuclei immediately before the collision, which makes it more interesting from a phenomenological point of view.

In other words, we have

$$\langle \rho(x, y) \rangle = \mathcal{N} \cdot T_A(x, y) \cdot T_B(x, y) \quad (11)$$

In this expression,  $T_A$  and  $T_B$  are the nuclear thickness functions for the incident and target nuclei, respectively, and are defined as the probability that a nucleon in nucleus A

is in position  $\vec{x} = (x, y)$ . We use this model because our analysis focuses on an average over multiple events and not on studying the behavior of an individual event.

It was used MUSIC [15] to calculate the  $K_n$ . This software uses the CGC model with a deformation in the spatial distribution of energy density, so that the code calculates the eccentricities and performs the hydrodynamic. That is, if we do N hydrodynamic simulations with the same input file, MUSIC will provide the same initial conditions (In other words, if we did not introduce deformation, we would have a completely symmetric system, i.e.,  $\epsilon_n = 0$  and  $v_n = 0$ ).

#### 3.1.1 Deformed CGC Model

This is a change made to the CGC model described in the previous section. This deformation consists of the addition of an asymmetry term called *stretch*. This treatment had already been proposed within MUSIC for a Gaussian profile of the initial energy density, as used by Franco et al. [5].

$$\text{stretch} = \sum_{n=2}^{N+1} \text{ecc}[n-1] \cdot \cos(n \cdot \phi - n \cdot \psi[n-1]); \quad (12)$$

In this equation,  $\text{ecc}[n-1] \equiv a_{n-1}$  represents the (n-1)-th spatial asymmetry term that is put *ad hoc* into the input file,  $\psi[n-1]$  is the angular asymmetry term, which was considered null in our simulations, and  $N$  is the maximum harmonic considered. The angle  $\phi$  is defined as  $\phi \equiv \arctg(\frac{y}{x})$ , and the index  $n$  can vary up to as many harmonics as we want to calculate, and, in our case, we use up to the 5th harmonic.

This term deforms the spatial distribution of energy density in the initial configuration of the system. To do this, it is added to the expression that determines the energy density distribution, and, in our case, it was added to the Woods-Saxon potential expression, which is the expression typically used to determine the approximate shape of the nucleus. Thus, we arrive at the following expression:

$$f(x, y, z) = \frac{\rho_0}{1 + e^{(\sqrt{(x^2+y^2) \cdot \text{stretch} + z^2} - R_0) / \chi}} \quad (13)$$

Then, this expression is used to calculate the thickness functions and the mean in the energy density distribution.

$$T(x, y) = \int_{-\infty}^{\infty} dz f(x, y, z) \quad (14)$$

$$\rho(x, y) \propto \mathcal{N} (T_A(x, y))^2$$

where  $\mathcal{N}$  is a normalization constant that determines the multiplicity of charged hadrons ( $\frac{dN_{ch}}{d\eta}$ ). We squared the thickness function, as the simulations were carried out with impact parameter  $b = 0$  and the two identical cores, as we are

concerned with the effects of fluctuations in symmetric collisions, so that the effects arising solely from fluctuations are more evident. Figure 2 illustrates the effect of adding the stretch term for each harmonic (e.g., for the first plot,  $a_n = 0$  for  $n \neq 2$  and  $a_2 = 0.1$ . For the second one,  $a_3 = 0.1$  and  $a_n = 0$  for  $n \neq 3$  and so on) and the effect of adding a term with all non-zero terms. In these graphs, we can observe the anisotropy in the distribution of energy density.

### 3.2 Obtaining $K_n(\frac{\eta}{s})$

As previously stated, in ultra-central events, there is a linear relationship between the initial conditions ( $\epsilon_n$ ) and the hydrodynamic response ( $v_n$ ). This can be seen in Fig. 3, obtained from simulations carried out in MUSIC.

In this work, it was assumed that the response coefficients  $K_n$  depend only on the shear viscosity  $\frac{\eta}{s}$  and that this parameter is constant throughout the evolution of the system. To determine the behavior of  $K_n$ , we carried out several simulations with different values for the normalization factor  $\mathcal{N}$  and different viscosities, in order to find a relationship between the factor  $\mathcal{N}$ , the multiplicity, and shear viscosity. In Fig. 4, the terms “ $f_n(x)$ ” in the legend represent the adjustments made for each viscosity value assigned in the input file. The results are illustrated in Fig. 4 where a logarithmic adjustment was made between  $\mathcal{N}$  and the multiplicity  $\frac{dN_{ch}}{d\eta}$ . Figure 5 shows the value of  $\mathcal{N}$  in terms of the viscosity  $\frac{\eta}{s}$  for  $\frac{dN_{ch}}{d\eta} = 2000$  [3]. As we can see in the same figure, the factor  $\mathcal{N}$  is inversely proportional to the shear viscosity. This fact was expected because multiplicity is proportional to viscosity. Therefore, to keep the multiplicity constant, we must decrease the value of the factor as the viscosity increases.

With the knowledge of this relationship, using a script written in bash, we carried out simulations in which the normalization factor was changed in order to keep the multiplicity of charged hadrons per unit of pseudorapidity ( $\frac{dN_{ch}}{f} \text{fixed} \eta$ ). This was done to highlight the relationship only between the flow (represented by the factor  $K_n \equiv \frac{v_n}{\epsilon_n}$ ) and the shear viscosity, as we see in Fig. 6, where  $\eta$  means the pseudorapidity [14] of emergent beam.

Table 1 displays the coefficients found when making a straight line adjustment, that is,  $K_n(\frac{\eta}{s}) = f_n \cdot \frac{\eta}{s} + g_n$ , for each harmonic for ATLAS

## 4 Constraining $\kappa_2$

To leading order in fluctuations, the RMS eccentricity (10) depends only on the mean and variance of the local energy

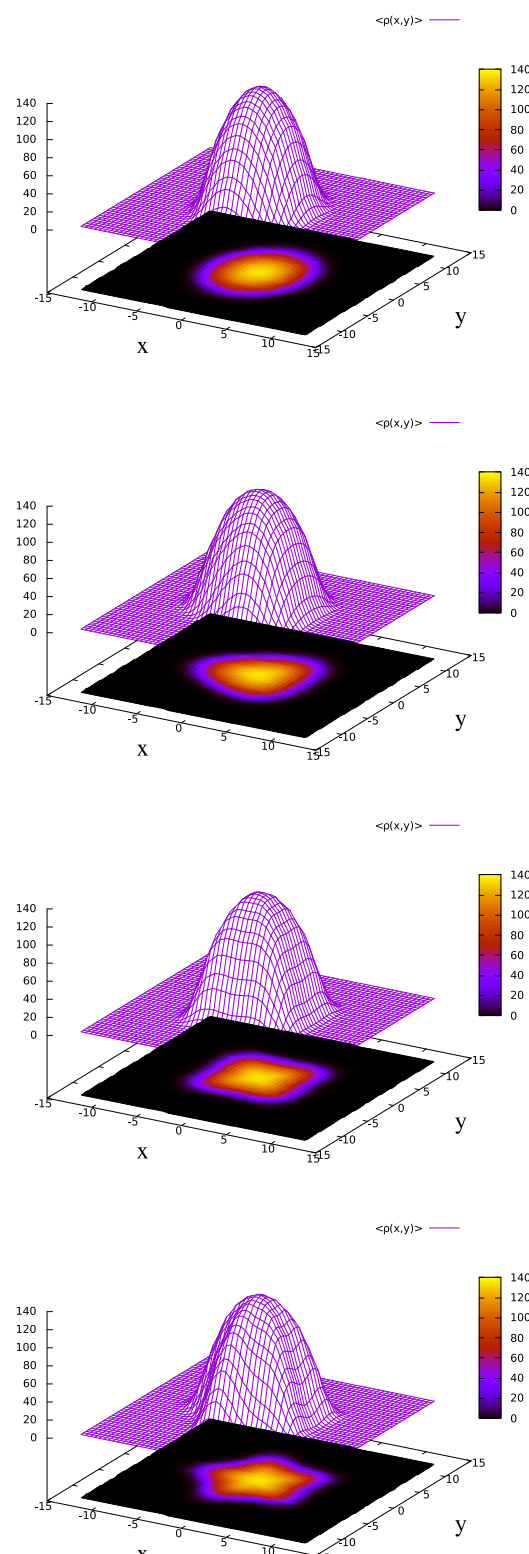
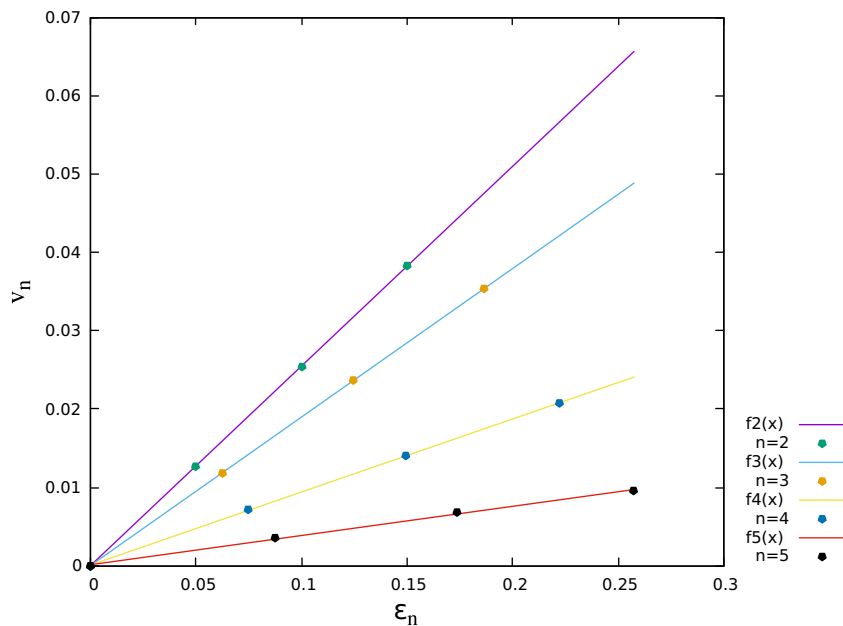


**Fig. 2** Energy density distribution using the deformed CGC model. We can observe the anisotropy in the energy density distribution for the different strain terms added and when all terms are non-zero

**Fig. 3** Relationship between  $v_n$  and  $\epsilon_n$  with results obtained using the deformed CGC model and with a linear adjustment over each harmonic, with  $f_2(x)$  being a linear adjustment between  $v_2$  and  $\epsilon_2$ ,  $f_3(x)$  an adjustment between  $v_3$  and  $\epsilon_3$ , and so on



fluctuations via functions  $\kappa_1$  and  $\kappa_2$ . Ultra-central collisions generally consist of collisions with small impact parameter, with spatial asymmetry dominantly generated by fluctuations. We therefore expect the average density  $\kappa_1$  to have approximate rotational symmetry, and only the radial falloff in density must be specified. Here, we take inspiration from the Color Glass Condensate [12] (as well as the Glauber wounded nucleon model) and assume an average energy density that is a product of nuclear thickness functions (i.e., the probability density for finding a nucleon at transverse position  $\vec{x}$ ). Since  $b \simeq 0$ , this reduces to a square of the nuclear

thickness function:

$$\kappa_1(\vec{x}) = \kappa_1(r_\perp) = N T_A^2(r_\perp) \quad (15)$$

$$T_A(\vec{x}) = T_A(r_\perp) = \int dz \frac{1}{1 + e^{(r-R)/a}} \quad (16)$$

where  $r = \sqrt{x^2 + y^2 + z^2}$ ,  $R = 6.62$  fm and  $a = 0.546$  fm are the radius and skin thickness of a Pb nucleus, respectively, and  $N$  is a normalization factor that depends on collision energy. Here, we omit the separate normalization factor in the definition of the thickness function  $T_A$  (nominally a

**Fig. 4** Multiplicity of charged hadrons as a function of the N factor adopted with the experimental cuts of the CMS collaboration, namely,  $0.3 < pT < 3.0$  GeV

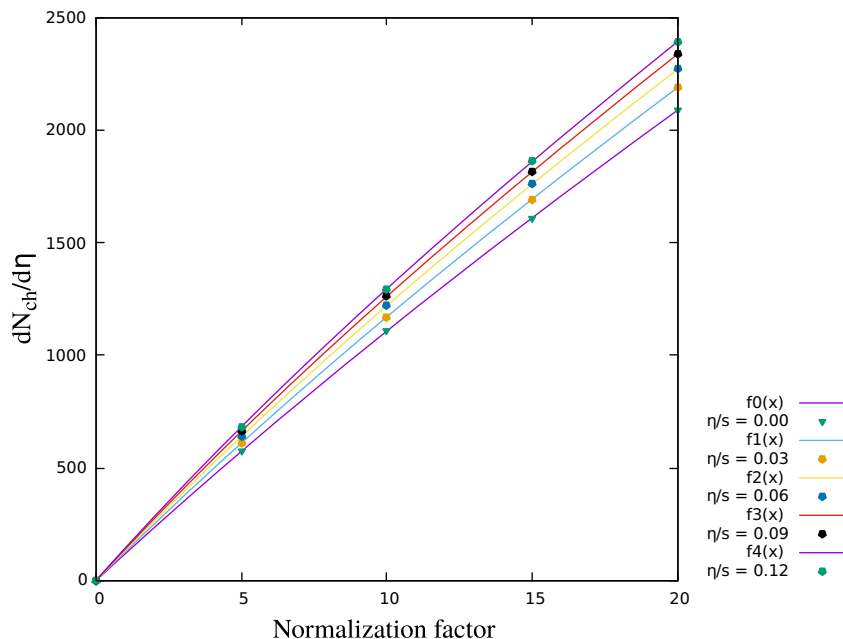
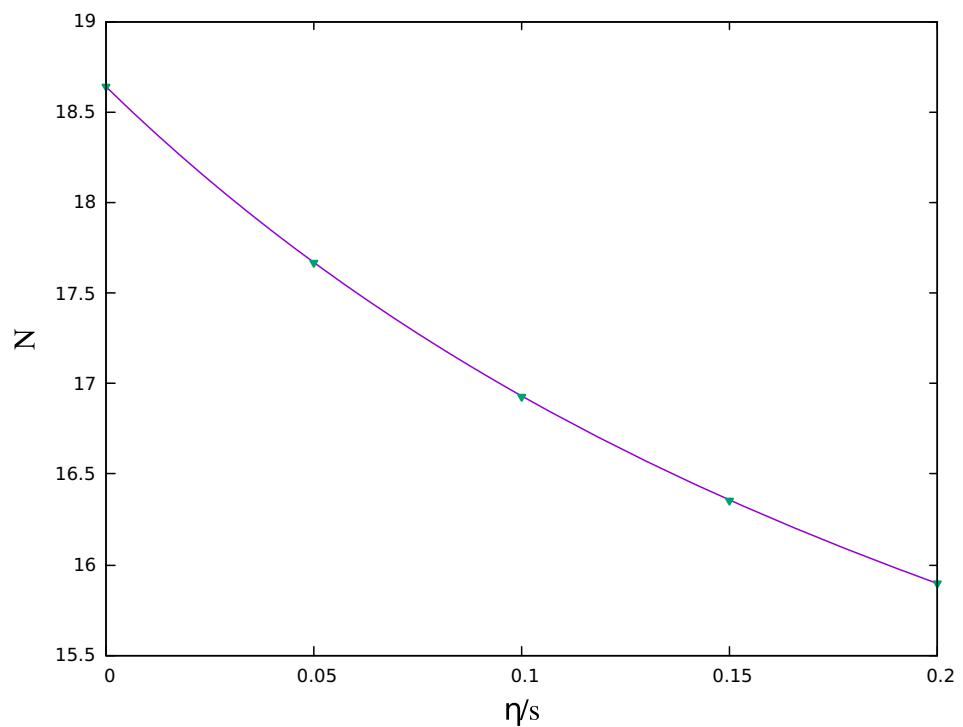


**Fig. 5** Factor  $N$  as a function of viscosity for  $\frac{dN_{ch}}{d\eta} = 2000$  with the same experimental cuts as in the previous graph



normalized probability density), so that it is absorbed into the constant  $N$ , which therefore has dimensions of energy density per unit area,  $E/L^5$ . Note that due to the strong initial longitudinal expansion, the energy density, and therefore  $N$ , also depends on the time when the density is being evaluated.

The main focus is on the fluctuations, encoded by  $\kappa_2(\vec{x})$ . Symmetry again dictates that it only depends on transverse radius  $r_\perp$ . Instead of parameterizing the radial dependence directly, it is perhaps more physically transparent to treat it

as a function of the local density. So we write  $\kappa_2$  as a parameterized function of  $\kappa_1$ , whose parameters we can constrain by comparison with data. Specifically, we write

$$\kappa_2(r_\perp) = C^2 N^{2-2p} \kappa_1(r_\perp)^{2p}. \quad (17)$$

For example, a Gaussian distribution has variance equal to the square of the mean and so would correspond to  $p = 1$ , and the Gamma distribution has  $p = 0.5$  because  $\kappa_2 \propto \kappa_1$ .

**Fig. 6** Response coefficient  $K$  in terms of shear viscosity  $\frac{\eta}{s}$  for a fixed value of eccentricities. Values calculated with the experimental cuts from the ATLAS collaboration, namely,  $|\eta| < 2.5$  e  $0.5 < pT < 3.0$

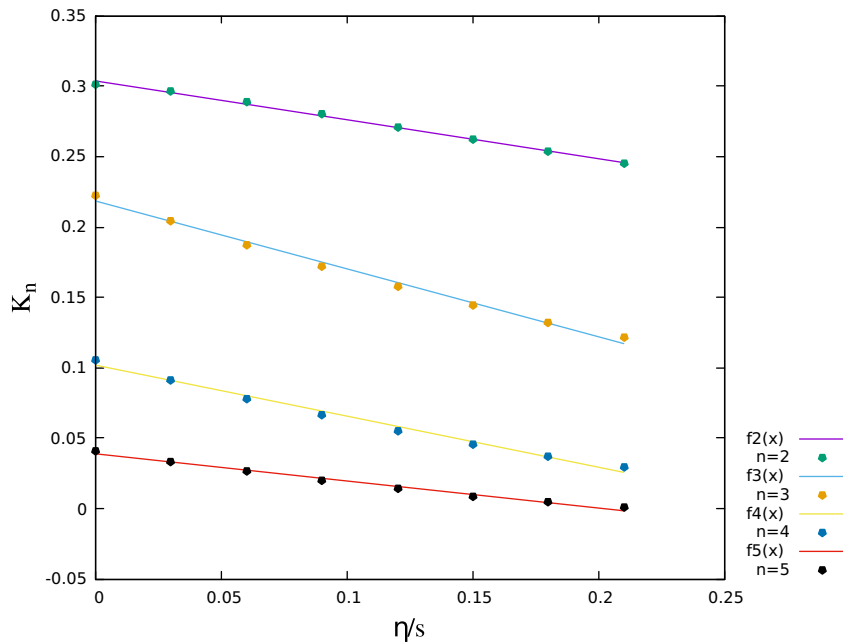


**Table 1** Angular  $f_n$  and linear  $g_n$  coefficients of the linear fit for each response coefficient to ATLAS 0 – 1% cent. bin

n	$f_n$	$g_n$
2	–0.276	0.304
3	–0.482	0.218
4	–0.362	0.102
5	–0.193	0.039

The parameter  $C$  (with non-integer dimension  $L^{10-4p}/E^2$ ) is defined for convenience so that it represents a multiplicative constant in the RMS eccentricity, and the parameter  $p$  encodes how the fluctuations depend on density (or equivalently, transverse radius)

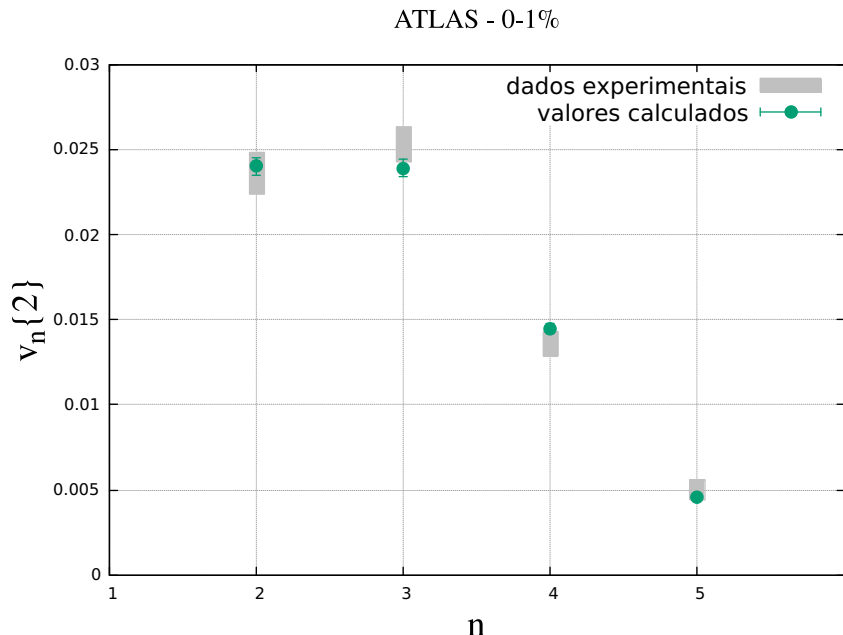
$$\varepsilon_n\{2\} = C \sqrt{\frac{\int d^2x r_\perp^{2n} (T_A)^{4p}}{(\int d^2x r_\perp^n T_A)^2}}. \quad (18)$$

It is important to highlight that the convenience of using (18) instead of obtaining the RMS eccentricity by numerical methods lies in the fact that we can identify, from this expression, the influence of fluctuations in the initial state on the final observables, since we start from the parameterization  $\kappa_2 = C^2 \kappa_1^{2p}$ .

## 5 Results

Now, the flow harmonics will be calculated using the n-point function method [9] and the least squares method [16] for comparison with experimental results (Fig. 7).

As shown in Fig. 6, the response coefficients  $K_n$  decrease with increasing viscosity, and this can be explained by

**Fig. 7** Experimental and calculated values of  $v_n\{2\}$ **Table 2** Values of  $p$ ,  $C$ ,  $\eta/s$ , their uncertainties, and  $\chi^2$  related to ATLAS 0 – 1%

$p$	$C$	$\sigma_C$	$\eta/s$	$\sigma_{\eta/s}$	$\chi^2_{dof}$	cent. bin
0.12	10.58	3.6	0.16	0.005	1.42	0 – 1%

remembering that increasing viscosity means a decrease in the interaction between particles, implying a decrease in the hydrodynamic behavior of the system. Thus, using the expressions of  $K_n(\eta/s)$  and the definitions of eccentricity from the 2-point function (Eq. 18), we obtain 4 equations:

$$v_2\{2\} = K_2 \cdot \varepsilon_2\{2\} \quad (19)$$

$$v_3\{2\} = K_3 \cdot \varepsilon_3\{2\} \quad (20)$$

$$v_4\{2\} = K_4 \cdot \varepsilon_4\{2\} \quad (21)$$

$$v_5\{2\} = K_5 \cdot \varepsilon_5\{2\} \quad (22)$$

From the knowledge of the factors  $K_n$ , we apply the least squares method, calculating the factor  $Q$ :

$$Q = \sum_{n=2}^5 (v_n^{exp}\{2\} - K_n(\eta/s) \cdot \varepsilon_n\{2\})^2 \cdot (\omega_n^{exp})^2, \quad (23)$$

where  $(\omega_n^{exp})^2$  is the inverse of the square of the uncertainties. Thus, from *ad hoc* values of the parameter  $p$ , we calculate the critical points for the unknown parameters, which in our case are the shear viscosity  $\eta/s$  and the factor  $C$  of proportionality between the mean and variance. In other words, the optimal value of  $p$  was achieved by trial and error, considering the following bonds to be physically valid:

**Table 3** Experimental and calculated values of  $v_n\{2\}$  with their respective uncertainties for ATLAS 0–1%

n	$v_n^{exp}$	$\sigma_{v_n}^{exp}$	$v_n^{calc}$	$\sigma_{v_n}^{calc}$
2	0.0236	0.00118	0.0240	0.00048
3	0.0253	0.00101	0.0239	0.00048
4	0.0137	0.00068	0.0145	0.00029
5	0.0047	0.00060	0.0046	0.00009

- The viscosity must be positive and have a small value, i.e.,  $\frac{\eta}{s} \ll 1$ . [13].
- $\chi^2$  must be small compared to other calculations already performed.<sup>2</sup>

$$\frac{\partial Q}{\partial(\frac{\eta}{s})} = 0 \quad (24)$$

$$\frac{\partial Q}{\partial C} = 0 \quad (25)$$

In order to get the results accuracy, we calculated  $\chi^2$

$$\chi^2 = \sum_{n=2}^5 (v_n^{exp}\{2\} - v_n^{calculated})^2 \cdot (\omega_n^{exp})^2 \quad (26)$$

Finally, it was calculated the parameter uncertainties to obtain the uncertainties of the calculated results, as it will be shown in Appendix A.

Thus, they have obtained the results for  $v_n\{2\}$  that are in Tables 2 and 3 and their parameters  $\eta/s$ ,  $C$ , and  $p$ , which are in Table 2.

## 6 Final Considerations

In this work, we study collisions in the ultra-central regime and tried to describe the experimental results from computer simulations. We implement the deformed CGC, with the addition of asymmetry terms in the mean density of energy. From this model, we verified the existence of a linear relationship between the initial conditions, represented by eccentricities  $\varepsilon_n\{2\}$  and the final conditions of the system, represented by flow harmonics  $v_n\{2\}$ .

This relationship obtained is approximately linear due to the fact that the collisions are in an ultra-central regime, where the eccentricities are small and arising from fluctuations. These fluctuations originate mainly from randomness

<sup>2</sup> In other words, the results calculated by the n-point function must be as close as possible to the experimental data.

from the position of the participating nucleons and due to quantum effects, and the latter are the responsible for event-to-event fluctuations, as seen in Giacalone et al. [7].

With this procedure and the use of the power parameterization (Eq. (17)), which establishes a direct relation between the energy density and their fluctuations, we got reasonable results for  $v_n\{2\}$  (i.e., accurate results related to the experimental values from [1]), and the values obtained for  $\frac{\eta}{s}$  are in agreement with previous works, such as Luzum et al. [13] and in Heinz et al. [10].

In future works, one can think of adding more parameters, as the bulk viscosity  $\zeta$  for instance, and assume a temperature dependence over the hydro parameters, by some parameterization, as proposed by JETSCAPE collaboration [4] in order to improve the presented results.

## Appendix A: Uncertainties of the Parameters

The parameters uncertainties are calculated from

$$(\mathcal{M}^{-1})_{jj} \quad (27)$$

With  $\mathcal{M}$  being an invertible matrix, defined by

$$\begin{bmatrix} \sum_{i=2}^5 \omega_i^2 f_I(v_i)^2 & \sum_{i=2}^5 \omega_i^2 f_I(v_i) f_{II}(v_i) \\ \sum_{i=2}^5 \omega_i^2 f_{II}(v_i) f_I(v_i) & \sum_{i=2}^5 \omega_i^2 f_{II}(v_i)^2 \end{bmatrix}$$

With  $f_I$  and  $f_{II}$  being the derivatives of the flow coefficient expressions, i.e.,

$$f_I(v_i) = \frac{\partial v_i}{\partial(\frac{\eta}{s})} \quad (28)$$

$$f_{II}(v_i) = \frac{\partial v_i}{\partial C} \quad (29)$$

The uncertainties about the parameters are given by  $(\mathcal{M}^{-1})_{jj} = \frac{1}{\text{Det}(\mathcal{M})} \cdot \text{cof}(\mathcal{M}_{jj})$ . Then,

$$\sigma_{\frac{\eta}{s}} = \frac{1}{\text{Det}(\mathcal{M})} \cdot (\mathcal{M}_{22}) \quad (30)$$

$$\sigma_C = \frac{1}{\text{Det}(\mathcal{M})} \cdot (\mathcal{M}_{11}) \quad (31)$$

Finally, the uncertainty about the fitted value of each harmonic  $v_n$  is calculated using the definition of error propagation [16].

$$\sigma(v_n) = \sqrt{(\frac{\partial v_n}{\partial(\frac{\eta}{s})} \sigma_{\frac{\eta}{s}})^2 + (\frac{\partial v_n}{\partial C} \sigma_C)^2} \quad (32)$$

**Author Contributions** The author wrote the entire text.

**Data Availability** No datasets were generated or analyzed during the current study.

## Declarations

**Conflict of interest** The author declares no Conflict of interest.

**Compliance with Ethical Statement** The author declares compliance with ethical statement.

**Ethical Conduct** The author declares ethical conduct.

## References

1. G. Aad et al., Measurement of the azimuthal anisotropy for charged particle production in  $\sqrt{s_{NN}} = 2.76$  TeV lead-lead collisions with the ATLAS detector. *Phys. Rev. C* **86**, 014907 (2012)
2. J.-P. Blaizot, W. Broniowski, J.-Y. Ollitrault, Continuous description of fluctuating eccentricities. *Phys. Lett. B* **738**, 166–171 (2014)
3. S. Chatrchyan et al., Dependence on pseudorapidity and centrality of charged hadron production in PbPb collisions at a nucleon-nucleon centre-of-mass energy of 2.76 TeV. *JHEP* **08**, 141 (2011)
4. D. Everett et al., Multisystem Bayesian constraints on the transport coefficients of QCD matter. *Phys. Rev. C* **103**(5), 054904 (2021)
5. R. Franco, M. Luzum, Rapidity-dependent eccentricity scaling in relativistic heavy-ion collisions. *Phys. Lett. B* **806**, 135518 (2020)
6. F.G. Gardim, F. Grassi, M. Luzum, J.-Y. Ollitrault, Mapping the hydrodynamic response to the initial geometry in heavy-ion collisions. *Phys. Rev. C* **85**, 024908 (2012)
7. G. Giacalone, P. Guerrero-Rodríguez, M. Luzum, C. Marquet, J.-Y. Ollitrault, Fluctuations in heavy-ion collisions generated by QCD interactions in the color glass condensate effective theory. *Phys. Rev. C* **100**(2), 024905 (2019)
8. A.V. Giannini, M.N. Ferreira, M. Hippert, D.D. Chinellato, G.S. Denicol, M. Luzum, J. Noronha, T. Nunes da Silva, J. Takahashi, Assessing the ultracentral flow puzzle in hydrodynamic modeling of heavy-ion collisions. *Phys. Rev. C* **107**(4), 044907 (2023)
9. H. Grönqvist, J.-P. Blaizot, J.-Y. Ollitrault, Non-Gaussian eccentricity fluctuations. *Phys. Rev. C* **94**(3), 034905 (2016)
10. U. Heinz, R. Snellings, Collective flow and viscosity in relativistic heavy-ion collisions. *Ann. Rev. Nucl. Part. Sci.* **63**, 123–151 (2013)
11. K. Kuroki, A. Sakai, K. Murase, T. Hirano, Hydrodynamic fluctuations and ultra-central flow puzzle in heavy-ion collisions. *Phys. Lett. B* **842**, 137958 (2023)
12. T. Lappi, Energy density of the glasma. *Phys. Lett. B* **643**, 11–16 (2006)
13. M. Luzum, J.-Y. Ollitrault, Extracting the shear viscosity of the quark-gluon plasma from flow in ultra-central heavy-ion collisions. *Nucl. Phys. A* **904–905**, 377c–380c (2013)
14. L. d. S. Santos, Estudo das flutuações em colisões ultracentrais de íons pesados relativísticos. PhD thesis, U. São Paulo (main) (2022)
15. B. Schenke, S. Jeon, C. Gale, (3+1)D hydrodynamic simulation of relativistic heavy-ion collisions. *Phys. Rev. C* **82**, 014903 (2010)
16. J. H. Vuolo, Fundamentos da Teoria de Erros. Edgard-Blucher (1996)

**Publisher's Note** Springer Nature remains neutral with regard to jurisdictional claims in published maps and institutional affiliations.

Springer Nature or its licensor (e.g. a society or other partner) holds exclusive rights to this article under a publishing agreement with the author(s) or other rightsholder(s); author self-archiving of the accepted manuscript version of this article is solely governed by the terms of such publishing agreement and applicable law.